



Asymmetric response of maximum and minimum temperatures to soil emissivity change over the Northern African Sahel in a GCM

Liming Zhou,^{1,2} Robert Dickinson,¹ Paul Dirmeyer,³ Haishan Chen,⁴ Yongjiu Dai,⁵ and Yuhong Tian⁶

Received 13 December 2007; revised 26 January 2008; accepted 31 January 2008; published 5 March 2008.

[1] Pronounced changes in land use and surface properties like those that have occurred in the Sahel could lead to reduced land surface emissivity and thus might have an asymmetric impact on daytime and nighttime surface air temperature. This paper analyzes the sensitivity of simulated climate and energy balance to changes in soil emissivity over the Sahel using the recently developed Community Land Model/Community Atmosphere Model. Model simulations indicate that the reduction of soil emissivity warms minimum temperature (T_{\min}) much faster than maximum temperature (T_{\max}) and thus decreases the diurnal temperature range (DTR) significantly. Lower emissivity reduces the outgoing longwave radiation and thus provides more energy to the atmosphere through increasing of sensible heat flux, ground and surface air temperatures. Statistical results show that, on average, a decrease of soil emissivity of 0.1 will increase T_{\min} by 0.55°C and 0.41°C, and decrease DTR by 0.59°C and 0.46°C under clear-sky and all-sky conditions, respectively, while T_{\max} changes little. The warming in T_{\min} and the decrease in DTR are much stronger during the dry season than the wet season and are higher in clear-sky conditions than all-sky conditions. These results suggest that changes in land surface emissivity over some particular regions might explain part of the observed decrease in DTR, especially over semi-arid regions.

Citation: Zhou, L., R. Dickinson, P. Dirmeyer, H. Chen, Y. Dai, and Y. Tian (2008), Asymmetric response of maximum and minimum temperatures to soil emissivity change over the Northern African Sahel in a GCM, *Geophys. Res. Lett.*, 35, L05402, doi:10.1029/2007GL032953.

1. Introduction

[2] Associated with global warming is a greater warming in minimum air temperature (T_{\min}) than maximum air temperature (T_{\max}), and thus a substantial reduction in the diurnal temperature range (DTR) observed over many land areas since 1950 [*Intergovernmental Panel on Climate*

Change (IPCC), 2007]. The decreasing trend of DTR has been linked to increases in cloud cover, soil moisture, greenhouse gases, and aerosols [*IPCC*, 2007]. Land cover/use changes can also decrease the DTR through modification of land surface properties over some regions [e.g., *Zhou et al.*, 2004, 2007; *Feddema et al.*, 2005]. Changes in land surface emissivity could be such an example. The land surface emissivity determines the amount of net thermal radiation absorbed by the surface and thus influences the surface radiation budget that controls important climate variables such as temperature [*Zhou et al.*, 2003, 2007; *Jin and Liang*, 2006]. Theoretical analyses and climate model sensitivity tests have demonstrated a strong diurnally asymmetric response of ground and air temperature to changes in surface emissivity over Northern Africa [*Zhou et al.*, 2003].

[3] The land surface emissivity decreases with the decreasing content of leaf area, leaf water, soil water, and soil organic matter [*Prabhakara and Dalu*, 1978; *Salisbury and D'Aria*, 1992; *Wilber et al.*, 1999]. Satellite observed surface emissivity is largely constant over dense vegetation but varies considerably over arid and semi-deserts [*Ogawa and Schmugge*, 2004; *Jin and Liang*, 2006]. Larger impacts of changes in surface emissivity on surface climate and energy balance, however, are possible over some particular regions where the surface properties are modified significantly as a notable temporal change may occur only over a long period. For example, the prolonged effects of drought, land degradation, soil erosion, and increased human activities may decrease the surface emissivity through reduced soil wetness, soil fertility, vegetative cover and productivity.

[4] *Zhou et al.* [2007] developed a new hypothesis based on GCM studies that a reduction in either soil emissivity and/or vegetation cover would act to increase T_{\min} much faster than T_{\max} and hence reduce the DTR - a mechanism possibly explaining some of the decrease in DTR observed in the Sahel since 1950s. According to this hypothesis, a reduction of vegetation cover and soil emissivity would have occurred during periods of drought and human mismanagement (e.g., overgrazing, overfarming, and deforestation). The former would increase daytime heat storage as a result of less shading of the underlying soil and hence more soil heating during nighttime. The latter would decrease longwave heat loss as a result of lower emissivity. Reducing vegetation cover also exposes more soil directly to the atmosphere, increasing the importance of the soil's lower emissivity on both the absorption and emission of longwave radiation. These changes allow for more energy to be transferred from the soil to the atmosphere via sensible heating, especially in dry stable boundary conditions, and significantly warm nighttime temperatures.

¹School of Earth and Atmospheric Sciences, Georgia Institute of Technology, Atlanta, Georgia, USA.

²Visiting Scientist at Center for Ocean-Land-Atmosphere Studies, Calverton, Maryland, USA.

³Center for Ocean-Land-Atmosphere Studies, Calverton, Maryland, USA.

⁴Jiangsu Key Laboratory of Meteorological Disaster, Nanjing University of Information Science and Technology, Nanjing, China.

⁵School of Geography, Beijing Normal University, Beijing, China.

⁶IMSG at NOAA/NESDIS, Camp Springs, Maryland, USA.

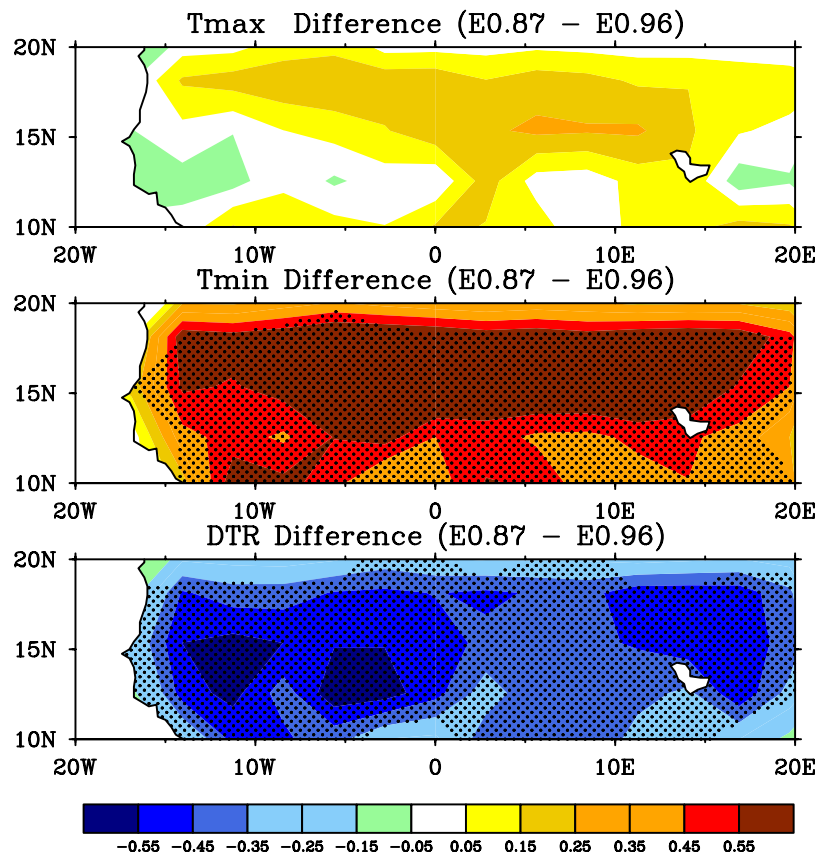


Figure 1. Spatial patterns of simulated annual mean 2 m surface air temperature (T_{\max} , T_{\min} , and DTR) differences ($^{\circ}\text{C}$) by decreasing the soil emissivity from 0.96 (E0.96) to 0.87 (E0.87) under clear-sky conditions in the Sahel. Stippling shows grid cells where the temperature differences are statistically significant at the 5% level. A two-tailed student's t test was used to test whether the difference differs significantly from zero.

[5] One quantitative uncertainty in this hypothesis is the unrealistic treatment of vegetation in GCMs. Vegetation and soil have separate emissivity values. They are combined essentially by geometric optics to determine what fraction of surface emission will penetrate the canopy. Climate models currently ignore such geometric effects by assuming that vegetation is homogeneous and thus can produce large errors in the estimation of surface radiation of semi-arid systems.

[6] To separate the impacts on the diurnal cycle of temperature of a reduction in vegetation cover versus that in soil emissivity, this study investigates further how changes in soil emissivity alone can modify T_{\max} , T_{\min} , and thus DTR. Unlike the study of Zhou *et al.* [2007] that considered an extreme case of a soil emissivity reduction by 0.07, here we have performed tests of sensitivity to a possible range of soil emissivity changes over the Sahel. In addition, we have used statistical analyses to quantify the magnitude of changes in T_{\max} , T_{\min} , and DTR as a function of soil emissivity.

2. Model and Experiments

[7] The latest Community Land Model (CLM3) coupled with the Community Atmosphere Model (CAM3) [Oleson *et al.*, 2004] was used to quantify the impacts of changes in soil emissivity on T_{\max} , T_{\min} , and DTR. CLM3 has been used as the land component of the Community Climate

System Model for extensive coupled climate model simulations contributed to the Intergovernmental Panel on Climate Change (IPCC). In CLM3, the soil emissivity is set as a constant value of 0.96, and the leaves and stems of vegetation are taken to have an emissivity of 1.0. For a vegetated patch in a model grid cell, the fraction of ground longwave radiation that is shaded locally by vegetation is modeled by $1 - e^{-LSAI}$, where $LSAI$ represents leaf and stem area index. The net longwave radiation flux over the land surface is calculated as a sum of fluxes for vegetation and its underlying ground. For non-vegetated surfaces ($LSAI = 0$), the flux is only from the ground.

[8] Our study region is located over the Sahel (10°N–20°N, 15°W–20°E) where a large reduction in soil emissivity may have occurred in the last several decades. To separate the vegetation impacts and exclude effects of uncertainties of vegetation versus soil radiation partitioning on our results, the vegetation over the Sahel was replaced by bare soil. Although this study focuses on quantifying the effect of soil emissivity changes on temperatures over non-vegetated regions, such an effect over vegetated regions should be proportional to the fraction of soil exposed directly to the atmosphere.

[9] Various estimates of satellite derived broadband emissivity (e.g., 8–14 μm) produced for use in climate models have ranged from 0.83 to 0.96 for arid and semi-arid regions [Zhou *et al.*, 2003; Ogawa and Schmugge, 2004; Jin and

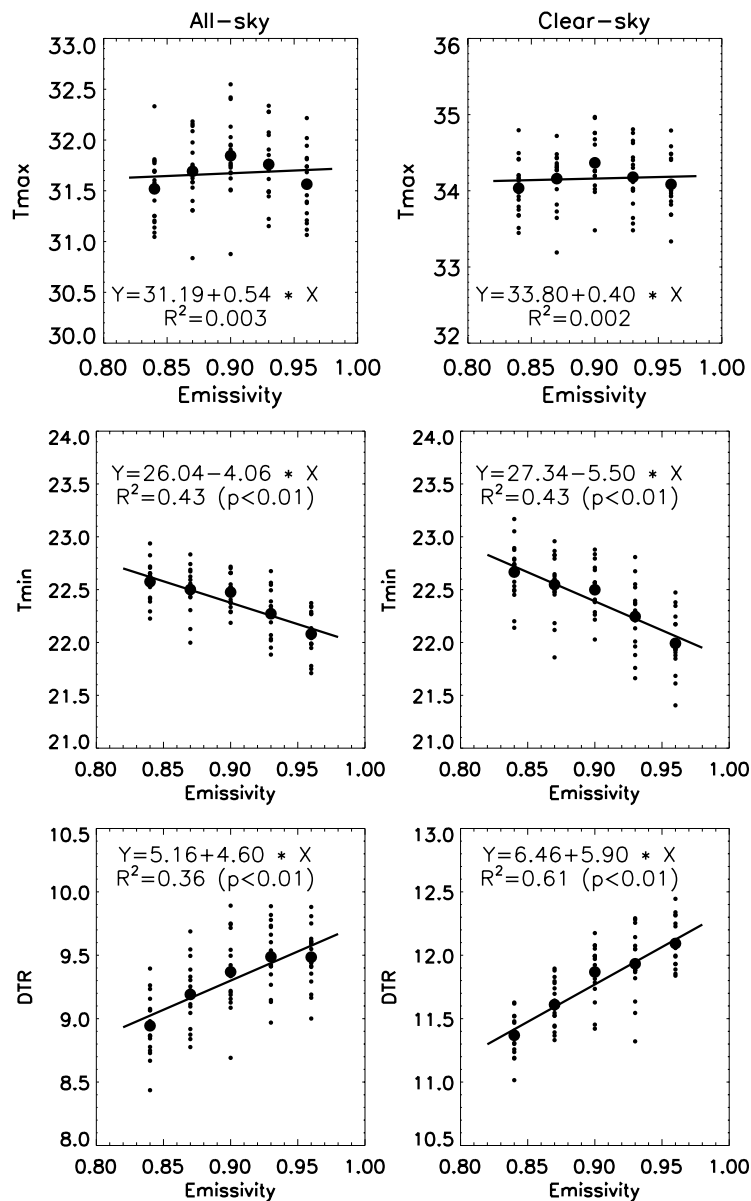


Figure 2. Changes in annual mean 2 m surface air temperature (T_{max} , T_{min} , and DTR) as a function of the soil emissivity of 0.84, 0.87, 0.90, 0.93, and 0.96 under clear-sky and all-sky conditions averaged in the Sahel. The smaller dot represents annual means and the larger dot represents the 18-year average. A linear regression was fit to each variable for the annual means, with a total of 90 samples (18 years \times 5 simulations), and its slope was estimated to assess how much the variable will change for a unit increase of soil emissivity. A two-tailed student's t test was used to test whether the slopes differ significantly from zero.

Liang, 2006], we assumed soil emissivity values of 0.84, 0.87, 0.90, 0.93, and 0.96, respectively, in our study region to test their impacts on climate and energy balance, while all other soil properties were unchanged. In total, five 20-year simulations were executed from CLM3/CAM3 at a resolution of about $2.8^\circ \times 2.8^\circ$. The observed climatological sea surface temperature and sea ice were used to exclude the impacts of their variability on our simulated temperature changes. The first 2 years of model runs were used as spin-up and the last 18-year results were analyzed in this study. Besides standard model outputs, we also examined 3 hour means for ground temperature, 2 m surface air temperature, longwave radiation, solar radiation, sensible heat, latent

heat, and soil flux. For each day, T_{max} and T_{min} were chosen from the eight simulated 2 m surface air temperatures. Regional averaging of model outputs was performed over the center of model grid cells ($11.2^\circ\text{--}16.7^\circ\text{N}$, $15.5^\circ\text{W}\text{--}19.7^\circ\text{E}$). Limiting the averaging to this region helps reduce impacts from surrounding land and ocean grid cells and allows the diurnal cycle of model variables to be composited with the model universal time (UT) calculation.

[10] As this study is focused on the soil emissivity impacts on DTR, most of our results are shown for clear-sky conditions, defined as the daily averaged low cloud cover less than 20%, to filter out any effects of changes in clouds and rainfall on simulated DTR. Another advantage

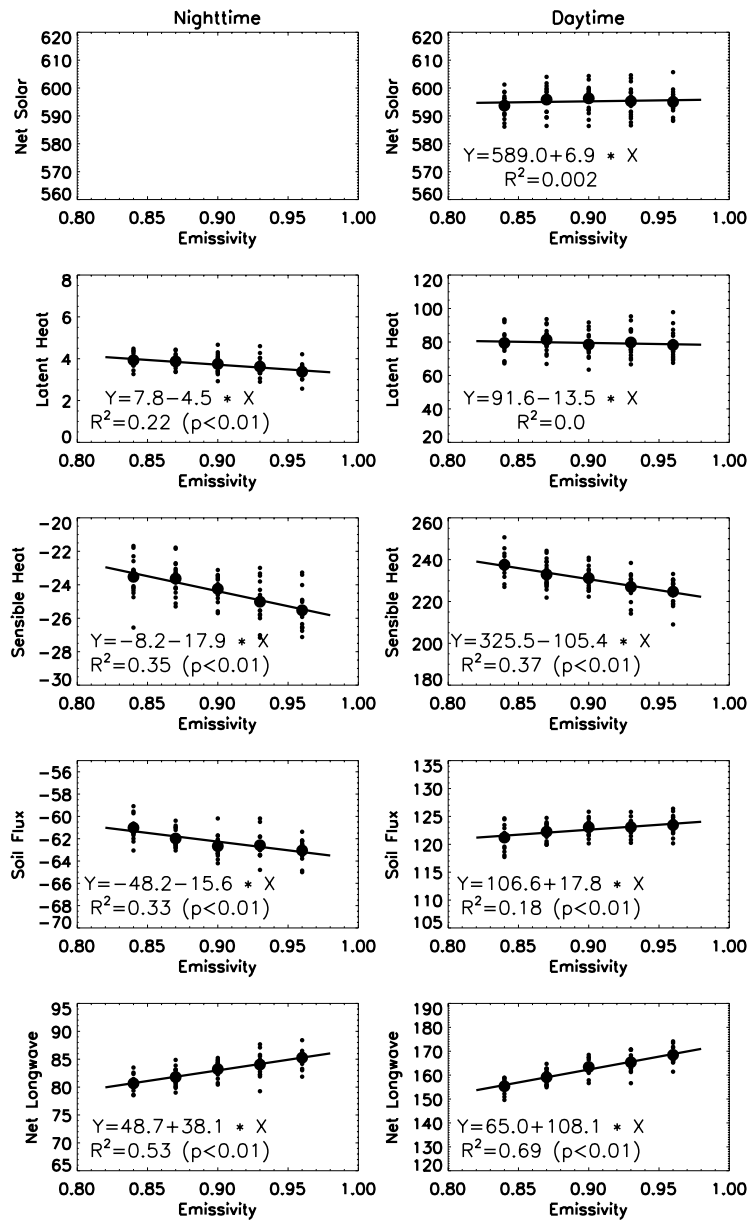


Figure 3. Same as Figure 2 but for changes in net solar flux, latent heat, sensible heat, soil flux, and net longwave radiation at daytime (UT 4–6 p.m.) and nighttime (UT 4–6 a.m.) in term of the model’s universal time (UT).

of conditioning the analysis by clear-sky is that it reduces impacts of uncertainties in modeled clouds and their long-wave radiation on DTR, especially during the wet season.

3. Results

[11] Figure 1 shows spatial patterns of differences in annual mean T_{max} , T_{min} , and DTR for the soil emissivity decreasing from 0.96 to 0.87 under clear-sky conditions. The reduction of soil emissivity causes a faster increase in T_{min} than in T_{max} . The simulated warming is strong and statistically significant for T_{min} over almost all the grid cells while the changes in T_{max} are small and insignificant, i.e., any changes in T_{max} are of the same magnitude as random variability. Consequently, the DTR declines significantly.

[12] Figure 2 shows how the regionally-averaged annual means of T_{max} , T_{min} , and DTR vary as a function of soil

emissivity increasing from 0.84 to 0.96. A linear regression is fit and its slope is estimated to assess how much the temperatures change for a unit change of emissivity. Evidently, DTR increases linearly with the increase of soil emissivity while T_{min} decreases and T_{max} is insensitive to the emissivity change. Regression results indicate that reducing the soil emissivity by 0.1 will increase T_{min} by $0.55^{\circ}C$ and $0.41^{\circ}C$, and decrease DTR by $0.59^{\circ}C$ and $0.46^{\circ}C$ under clear-sky and all-sky conditions, respectively.

[13] To examine changes in radiation and energy budget, Figure 3 shows how regionally averaged annual means of net solar radiation, net longwave radiation, latent heat, sensible heat, and soil fluxes vary as a function of soil emissivity increasing from 0.84 to 0.96 under clear-sky conditions. Since these variables vary diurnally, results are shown at daytime (UT 4–6 p.m.) and nighttime (UT 4–6 a.m.). Note that the net longwave radiation, net solar radiation, sensible

Table 1. Diurnal Cycle of Estimated Slopes for Temperatures and Radiation and Energy Budget As a Function of Soil Emissivity Averaged Over the Sahel^a

Variables	All-sky			Clear-Sky		
	JFM	JAS	Annual	JFM	JAS	Annual
<i>Nighttime (UT 4–6 a.m.)</i>						
Downward longwave radiation, W/m ²	17.3	–0.7	9.7	18.1	–3.7	16.7
Upward longwave radiation, W/m ²	61.0	13.2	40.6	61.4	37.6	54.8
Net longwave radiation, W/m ²	43.7	14.0	30.9	43.2	41.3	38.1
Latent heat, W/m ²	–1.8	–7.0	–6.6	–1.4	–8.3	–4.5
Sensible heat, W/m ²	–22.1	–1.2	–13.2	–22.0	–16.2	–18.0
Soil flux, W/m ²	–19.7	–5.8	–11.1	–19.8	–16.7	–15.6
Downward solar radiation, W/m ²	-	-	-	-	-	-
Net solar radiation, W/m ²	-	-	-	-	-	-
Ground temperature, °C	–8.1	–1.0	–5.2	–8.1	–3.0	–7.1
2 m surface air temperature, °C	–5.9	–0.8	–3.8	–5.8	–1.9	–5.2
<i>Daytime (UT 4–6 p.m.)</i>						
Downward longwave radiation, W/m ²	52.7	6.8	36.9	53.3	25.9	53.4
Upward longwave radiation, W/m ²	181.9	41.2	122.1	181.5	104.3	161.5
Net longwave radiation, W/m ²	129.2	34.4	85.2	128.2	78.4	108.1
Latent heat, W/m ²	–19.3	16.6	–30.0	–10.6	–21.9	–13.5
Sensible heat, W/m ²	–122.9	–1.2	–60.5	–127.8	–28.7	–105.4
Soil flux, W/m ²	29.3	13.9	18.2	28.3	3.0	17.8
Downward solar radiation, W/m ²	22.8	75.1	20.4	24.0	40.4	10.7
Net solar radiation, W/m ²	16.3	63.4	12.8	18.0	30.8	6.9
Ground temperature, °C	–2.3	0.5	–1.5	–2.5	–1.3	–3.0
2 m surface air temperature, °C	1.2	0.2	0.4	1.1	0.2	0.2

^aThe slopes were estimated as done in Figures 2–3, and their values in bold are statistically significant at the 5% level (a two-tailed student's *t* test was used as done in Figures 2–3). They represent how much the variables change for a unit increase of soil emissivity. JFM, January–February–March; JAS, July–August–September. The net longwave radiation, net solar radiation, sensible heat, and latent heat are defined as positive toward the atmosphere, and the soil flux is defined positive toward the ground. The temperatures and radiation and energy budget were 3-hour averages from each model time step (20 minutes) in term of the model universal time (UT).

heat, and latent heat are defined as positive toward the atmosphere, and the soil flux is defined positive into the ground. Evidently, the net solar radiation and the latent heat change little with the modification of soil emissivity, while the sensible heat, soil flux, and net longwave radiation have statistically significantly changed ($p < 0.01$). For a decrease of soil emissivity by 0.1, the net longwave radiation decreases by 3.8 W/m² and 10.8 W/m² at nighttime and daytime, respectively. Note that the net longwave radiation is defined as positive toward the atmosphere, so its decrease suggests less thermal emission and thus more radiation for sensible and soil fluxes. Consequently, the sensible heat increases by 1.8 W/m² and 10.5 W/m² during nighttime and daytime, respectively, and the soil heating is 1.6 W/m² at nighttime and the soil heat storage is 1.8 W/m² at daytime. The reduced thermal emission is mainly balanced by the increased sensible heat flux to the atmosphere.

[14] We calculated regionally averaged seasonal means of air and ground temperature, solar radiation, longwave radiation, sensible heat, latent heat, and soil heat fluxes and then estimated their slopes (Table 1) as done in Figures 2–3 for daytime (UT 4–6 p.m.) and nighttime (UT 4–6 a.m.). Our discussion below will focus on clear-sky conditions as the results under all-sky conditions can be explained similarly. During nighttime, the reduction of soil emissivity by 0.1 decreases the net longwave radiation by 4.3 W/m² in dry seasons (January–February–March) and 4.1 W/m² in wet seasons (July–August–September), mainly resulting from the reduction of upward longwave radiation, while the solar radiation changes little. Such change in the net radiation is mainly balanced by an increase of sensible heat flux by 2.2 W/m², latent heat

flux by 0.1 W/m², and soil heating by 2.0 W/m² in winter, and by an increase of sensible heat by 1.6 W/m², latent heat by 0.8 W/m², and soil heating by 1.7 W/m² in summer. Consequently, the ground and surface air temperature increase by 0.81°C and 0.58°C in winter and by 0.30°C and 0.19°C in summer, respectively. During daytime, the changes in net longwave radiation, sensible heat, and soil fluxes are much larger than those during nighttime and are statistically significant, while the latent heat and solar flux change insignificantly. The ground and air temperatures, however, change little compared to those during nighttime. Note that the downward longwave radiation decreases due to changes in the vertical distribution of water vapor and atmospheric temperature, possibly in response to the surface warming and the reduced upward longwave radiation from the ground.

[15] The simulated warming in ground and surface air temperature and the resulting decrease in DTR are much stronger in the dry season than in the wet season and are larger under clear-sky conditions than all-sky conditions (Table 1). The seasonal difference indicates that the warming due to the reduction of soil emissivity can be largely masked by the effects of increased ground evaporation and clouds in the wet season. In summer, the larger evaporation cools the surface and the larger cloud amounts sharply reduce solar heating during daytime. Consequently, less energy goes towards increasing surface temperatures. The day-night difference indicates that the reduction of soil emissivity warms nighttime temperature more than daytime temperature. For a given radiative forcing, a smaller impact on daytime temperature is expected because daytime turbulent mixing is stronger and a large

portion of the forcing is converted into latent heat through evapotranspiration.

4. Discussion

[16] This paper analyzes the sensitivity of simulated climate and energy balance to changes in soil emissivity over the Sahel, and considers how this information may be used to explain part of the observed DTR decline since 1950s. Our sensitivity tests show that there is generally a linear relationship between changes in soil emissivity and changes in ground and surface air temperature, net and upward longwave radiation, and sensible heat flux.

[17] Our results indicate that a reduction of soil emissivity could increase T_{\min} much more than T_{\max} and thus decrease the DTR over the Sahel. Since spatial and temporal variations of surface emissivity are small over most regions, such an effect might be significant only over some particular regions where the emissivity change has been substantial and evapotranspiration is limited. For example, Zhou *et al.* [2007] propose that soil aridation and vegetation removal due to drought and human mismanagement over the Sahel may have contributed to part of the observed long-term DTR reduction. As both observations and GCMs suggest an increased frequency and severity of drought in a warming climate [e.g., Dai *et al.*, 2004; Held *et al.*, 2006], the effect of drought could be amplified, especially over semi-arid regions where ecosystems, water quality, and soil fertility could be largely degraded by increasing human demand and mismanagement. These changes may modify the land surface emissivity sufficiently to cause a reduction in DTR. Changes in land surface properties such as desertification and urbanization might have a similar effect on DTR.

[18] One uncertainty in our assessments is the model's overestimation of soil evaporation [Dickinson *et al.*, 2006; Zhou *et al.*, 2007]. There is no significant change in the simulated precipitation after the vegetation removal. However, the excessive evaporation in our simulations will increase latent heat and decrease Bowen ratio which in fact would weaken our simulated DTR reduction during the wet season from the reduction in soil emissivity shown previously. Considering other model uncertainties and limitations, especially those describing mechanisms within the boundary layer treatment, further quantifications using other GCMs and validation with observations are needed.

[19] **Acknowledgments.** This study was supported by the NSF grant ATM-0720619 and the DOE grant DE-FG02-01ER63198. H. Chen was supported by the National Natural Science Foundation of China under grant 40405018 and the Foundation of Jiangsu Key Laboratory of Meteorological

Disaster (KLME050205), NUIST, China. Y. Dai was supported by the National Natural Science Foundation of China under grant 40225013 and the 111 Project of Ministry of Education and State Administration for Foreign Experts Affairs of China.

References

- Dai, A., K. E. Trenberth, and T. Qian (2004), A global data set of Palmer Drought Severity Index for 1870–2002: Relationship with soil moisture and effects of surface warming, *J. Hydrometeorol.*, **5**, 1117–1130.
- Dickinson, R. E., K. W. Oleson, G. Bonan, F. Hoffman, P. Thornton, M. Versteinstein, Z.-L. Yang, and X. Zeng (2006), The Community Land Model and its climate statistics as a component of the Community Climate System Model, *J. Clim.*, **19**, 2302–2324.
- Feddema, J. J., K. W. Oleson, G. Bonan, L. O. Mearns, L. E. Buja, G. A. Meehl, and W. M. Washington (2005), The importance of land cover change in simulating future climates, *Science*, **310**, 1674–1678.
- Held, I. M., T. L. Delworth, J. Lu, K. L. Findell, and T. R. Knutson (2006), Simulation of Sahel drought in the 20th and 21st centuries, *Proc. Natl. Acad. Sci. U. S. A.*, **103**, 1152–1153.
- Intergovernmental Panel on Climate Change (IPCC) (2007), *The IPCC Fourth Assessment Report: Climate Change 2007: The Physical Science Basis*, Cambridge Univ. Press, Cambridge, U. K.
- Jin, M., and S. Liang (2006), Improving land surface emissivity parameter of land surface models in GCM, *J. Clim.*, **19**, 2867–2881.
- Ogawa, K., and T. Schmugge (2004), Mapping surface broadband emissivity of the Sahara Desert using ASTER and MODIS data, *Earth Interact.*, **8**. (Available at <http://EarthInteractions.org>)
- Oleson, K. W., et al. (2004), Technical description of the Community Land Model (CLM), *NCAR Tech. Note NCAR/TN-461+STR*, 173 pp., Natl. Cent. For Atmos. Res., Boulder, Colo.
- Prabhakara, C., and G. Dalu (1978), Remote sensing of the surface emissivity at 9 μm over the globe, *J. Geophys. Res.*, **81**, 3719–3724.
- Salisbury, J. W., and D. M. D'Aria (1992), Emissivity of terrestrial materials in the 8–14 μm atmospheric window, *Remote Sens. Environ.*, **42**, 83–106.
- Wilber, A. C., D. P. Kratz, and S. K. Gupta (1999), Surface emissivity maps for use in satellite retrievals of longwave radiation, *NASA Tech. Pap., NASA/TP-1999-209362*.
- Zhou, L., R. E. Dickinson, Y. Tian, M. Jin, K. Ogawa, H. Yu, and T. Schmugge (2003), A sensitivity study of climate and energy balance simulations with use of satellite-derived emissivity data over Northern Africa and the Arabian Peninsula, *J. Geophys. Res.*, **108**(D24), 4795, doi:10.1029/2003JD004083.
- Zhou, L., R. E. Dickinson, Y. Tian, J. Fang, Q. Li, R. K. Kaufmann, C. J. Tucker, and R. B. Myneni (2004), Evidence for a significant urbanization effect on climate in China, *Proc. Natl. Acad. Sci. U. S. A.*, **101**, 9540–9544.
- Zhou, L., R. E. Dickinson, Y. Tian, R. Vose, and Y. Dai (2007), Impact of vegetation removal and soil aridation on diurnal temperature range in a semiarid region: Application to the Sahel, *Proc. Natl. Acad. Sci. U. S. A.*, **104**, 17,937–17,942.
- H. Chen, Jiangsu Key Laboratory of Meteorological Disaster, Nanjing University of Information Science and Technology, Nanjing 210044, China.
- Y. Dai, School of Geography, Beijing Normal University, Beijing 100875, China.
- R. Dickinson and L. Zhou, School of Earth and Atmospheric Sciences, 311 Ferst Drive, Georgia Institute of Technology, Atlanta, GA 30332, USA. (lmzhou@eas.gatech.edu)
- P. Dirmeyer, Center for Ocean-Land-Atmosphere Studies, Calverton, MD 20705, USA.
- Y. Tian, IMSG at NOAA/NESDIS, 5200 Auth Road, Camp Springs, MD 20746, USA.